

Evaluation of dual polarization radar for rainfall–runoff modelling: a case study in Sydney, Australia

PHILLIP JORDAN, ALAN SEED, PETER MAY & TOM KEENAN

Bureau of Meteorology, PO Box 1289K, Melbourne, Victoria 3001, Australia
p.jordan@bom.gov.au

Abstract Dual polarization radars have advantages that may translate into more accurate measurements of rainfall than are provided by conventional, single polarization radars. An investigation was performed into how much additional benefit will be delivered to practical rainfall–runoff modelling by dual polarization radar over the single polarization radar approach. The benefit of dual polarization is compared against the impact of using calibration raingauge networks for single polarization radar rainfall. The investigation is framed in the context of a case study: a widespread rainfall event of approximately 2 days duration producing a small flood in a partially urbanized basin of 354 km² area.

Key words dual polarization radar; single polarization radar; URBS rainfall–runoff model

INTRODUCTION

The application of meteorological radars to quantitative rainfall measurement and hydrological forecasting is increasing. Radar has obvious advantages for rainfall estimation in hydrology: detailed spatial and temporal resolution over an extensive spatial domain, collected by a single remote device, with the ability to make informed nowcasts of future rainfall. However, limitations on the accuracy of conventional single polarization radar in rainfall measurement have been acknowledged for some time. Commonly recognized sources of error include beam blockage, ground detection, hail contamination, variations in raindrop size distribution, attenuation, the vertical profile of reflectivity, wind induced drift, and effects of spatial and temporal sampling (see for example Austin, 1987; Harrold *et al.*, 1974; Jordan *et al.*, 2000).

Over the past decade, significant progress has been made in radar rainfall measurement using dual polarization radar. Signals returned by the horizontal and vertical polarized beams provide additional parameters that can be combined into a multi-parameter estimate of rainfall intensity. Multi-parameter rainfall estimates should: (a) be less susceptible to variations in the power of the radiation emitted by the radar; (b) reduce the impact of variations in rain drop size distribution; (c) be much less affected by attenuation of the rainfall beam as it passes through areas of rainfall; and (d) be much less affected by blocking of the radar beam by the surrounding terrain, which allows the beam to scan at lower elevations (Zrnić & Ryzhkov, 1996).

Hydrologists aim to make the best use of the available radar data while recognizing its shortcomings. Evaluation the accuracy of rainfall–runoff model forecasts made using radar data is a major step in this process (Carpenter *et al.*, 2001)

and there have been many studies that have applied single polarization radar rainfall data to rainfall–runoff models (see Borga, 2002 for a recent list). There are just two case studies in the literature that apply dual polarization radar data to flood forecasting. The papers by Ogden *et al.* (2000) and Yates *et al.* (2000) each considered flooding caused by intense convective thunderstorms on basins of 25 and 130 km², respectively. In each case study there was evidence that the dual polarization radar rainfall measurements produce more accurate modelled hydrographs than single polarization radar. However, in each study the hydraulic conductivity parameter, which has significant control on modelled runoff generation, was calibrated to the particular event to improve the rainfall–runoff model results.

Numerous studies (starting with Brandes, 1975) have shown that a network of reporting raingauges can successfully reduce the bias in radar rainfall estimates. Raingauge calibration of a reflectivity based rainfall accumulation field is an alternative or complement to a dual polarization approach. The cost of the calibration network obviously increases with its density.

This paper investigates how much additional benefit will be delivered to rainfall–runoff modelling by dual polarization radar over the conventional single polarization radar approach. The benefit of dual polarization is compared against the impact of using calibration raingauge networks of varying density. The investigation is framed in the context of a case study: a widespread rainfall event of approximately 2 days duration producing a small flood in a partially urbanized basin of 354 km² area.

STUDY BASIN AND INSTRUMENTATION

The Georges River basin is located approximately 30 km southwest of Sydney city, Australia. It drains in a roughly south to north direction to Liverpool Weir (33.925°S, 150.925°E). Upper reaches of the Georges basin are forested or partially cleared rural land and the lower reaches are urbanized (approximately 19% of the total basin area) with low-density industrial and residential development. Mean annual rainfall is 870 mm, with flood producing rainfall possible in any month of the year. An automatic water level recorder has been installed at Liverpool Weir since 1968 and the maximum recorded streamflow is 540 m³ s⁻¹.

The Bureau of Meteorology Research Centre (BMRC) operates a C-Band polarimetric (C-POL) radar (Keenan *et al.*, 2001) that was located at Badgery's Creek (33.894°S, 150.725°E), between 12 and 48 km northwest of the Georges River basin (see Fig. 1). The radar transmits radiation with a wavelength of 5.5 cm and produces a beam with a 3 dB width of 1°. C-POL measures several raw data fields including horizontal reflectivity (Z_h), differential reflectivity (Z_{dr}), differential phase shift (Φ_{dp}) and zero lag cross-correlation coefficient (ρ_{hv}). C-POL was operated in volume-scan mode, collecting data from 15 elevation angles every 10 min. The data resolution was 1.0° in azimuth and 300 m in range.

Raingauge data were obtained from 128 tipping bucket rainfall stations that are located within 105 km of C-POL. Tipping bucket sizes vary across the network between 0.2, 0.5 and 1.0 mm. The spatial distribution of raingauges is non-uniform, with none over the Pacific Ocean (east of the radar) and none in parts of the Blue Mountains (to the west). Therefore, the effective area of coverage of the gauge

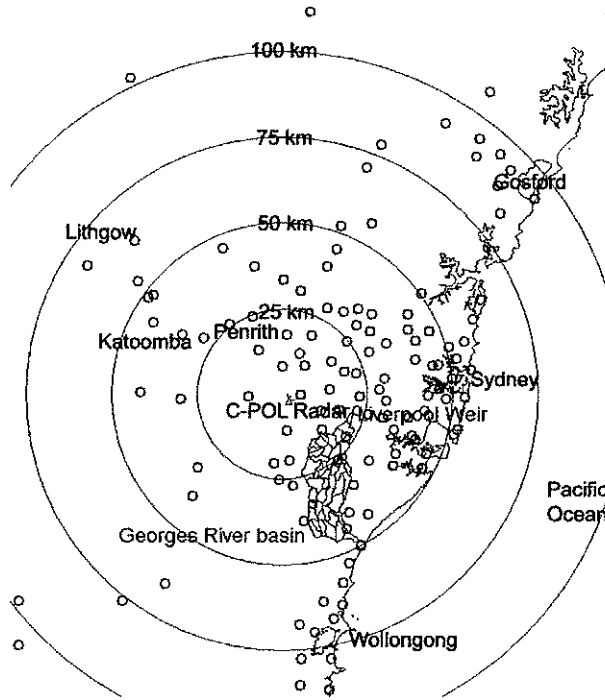


Fig. 1 Map showing area surrounding the C-POL radar, including the outline of the Georges River basin, the sub-areas of its URBS model, and the 128 raingauge network (small circles).

network is approximately 19 000 km² (see Fig. 1). This represents a raingauge network density of about 1 per 150 km². Less dense raingauge networks were simulated by randomly selecting gauges from the full network.

The Australian Bureau of Meteorology provides a flood warning service for the Georges River. Flood forecasts are made using the URBS rainfall–runoff routing model. The URBS model (Carroll, 1996) subdivides the Georges River basin along ridges in the topography into 47 sub-areas of similar area (as shown in Fig. 1), each represented by a rainfall-input node. Non-linear storages are used to represent the sub-area routing response, with the storage–discharge equation for each subarea given by:

$$S_{sa} = \beta \sqrt{AQ^m} \tag{1}$$

where S_{sa} is the sub-area storage volume, β is the sub-area lag parameter, A is the area of the sub-area, Q is the outflow from sub-area and m is the sub-area nonlinearity parameter.

URBS connects the sub-area storages using channel segments, with flows routed using the linear storage–discharge equation:

$$S_{ch} = \alpha L [xQ_u + (1-x)Q_d] \tag{2}$$

where S_{ch} is the channel storage volume, α is the channel lag parameter (the inverse of average flood wave speed), L is the length of reach, Q_u is the inflow to the upstream

Table 1 Calibrated parameter values for the Georges River basin URBS model.

Parameter name	Value
Model time step	60 min
Channel lag parameter, α	0.2448
Channel translation parameter, x	0.3
Sub-area lag parameter, β	3.473
Sub-area nonlinearity parameter, m	0.8
Impervious area	50% of urban area
Volumetric runoff coefficient (Impervious areas)	1.0
Volumetric runoff coefficient (Pervious areas)	0.2237

end and Q_d is the outflow from the downstream end of the reach and x is the translation parameter. A simple initial loss-proportional loss model is used to determine runoff generation from pervious areas. The semi-distributed nature of URBS allows for the spatial variability in the rainfall pattern to be utilised in prediction of flood hydrographs.

The URBS model for the Georges River basin was calibrated to five small flood events that occurred between November 2000 and March 2001. The floods varied in duration between 1 and 5 days and had peak flows of between 29 and 88 $\text{m}^3 \text{s}^{-1}$. Model parameters were calibrated using data from the raingauge network (with a density of 1 per 300 km^2) and the streamflow gauge at Liverpool Weir. The calibrated parameter values, shown in Table 1 were obtained using the shuffled complex evolution optimization algorithm (Duan *et al.*, 1992). The initial loss from pervious areas was calibrated independently for each of the five calibration events.

MODELLING APPROACH

A widespread rainfall system passed over the domain of C-POL from 19 April 2001 06:00 UTC to 22 April 2001 15:00 UTC. This system produced rainfall accumulations over the Georges basin of between 40 and 70 mm, with the most common rainfall intensities being less than 5 mm h^{-1} . A small flood event occurred in the Georges River, with a peak flow of 22.5 $\text{m}^3 \text{s}^{-1}$ recorded at 21 April 2001 23:00 UTC. The total recorded runoff is 2150 Ml, which represents average runoff from the basin of 6.08 mm.

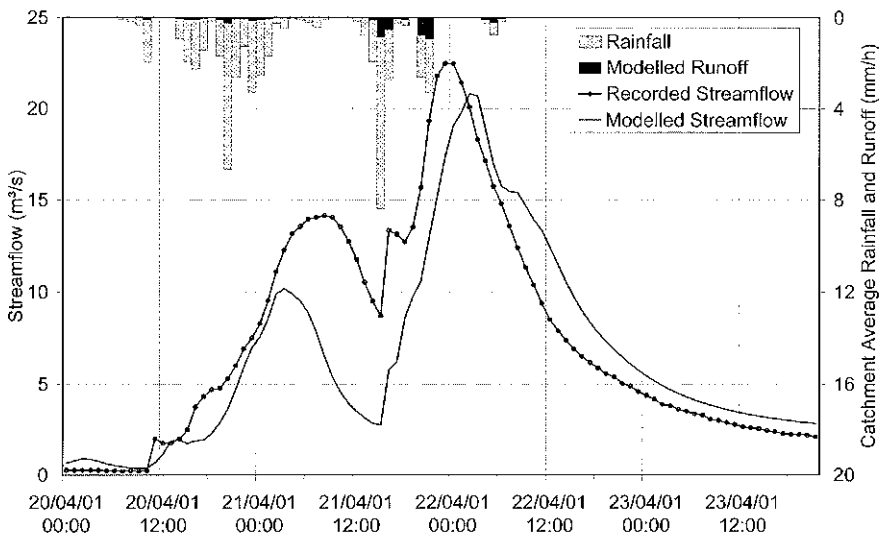
Six different algorithms were used to estimate rainfall intensity fields, as listed in Table 2. The first algorithm is a conventional $R(Z_{hS})$ relationship for convective precipitation where Z_{hS} is the reflectivity at horizontal polarization that was determined after carrying out quality control using the single polarization data only and attenuation correction using the Hitschfeld & Bordan (1954) method. The second algorithm, $R(Z_{hD})$, uses the same rainfall intensity estimation algorithm but it uses Z_{hD} , which is the reflectivity at horizontal polarization that was determined using the dual polarization radar data. In the $R(Z_{hD})$ algorithm, a threshold was applied on the ρ_{hv} field of 0.95 to identify probable areas of ground clutter, anomalous propagation and non-liquid precipitation and then the self-consistent rain profiling method (Bringi *et al.*, 2001) was used to perform attenuation correction on the reflectivity data. The four

Table 2 Equations for radar rainfall estimation algorithms.

Algorithm	Equation
$R(Z_{hs})$	$R = 0.015Z_{hs}^{0.734}$
$R(Z_{hd})$	$R = 0.015Z_{hd}^{0.734}$
$R(A_h)$	$R = \begin{cases} 243.2A_h^{0.79} & Z_{hd} > 35 \text{ dBZ and } A_h > 0 \text{ dBZkm}^{-1} \\ 0.015Z_{hd}^{0.734} & \text{otherwise} \end{cases}$
$R(A_h, Z_{dr})$	$R = \begin{cases} 677.1A_h^{0.96}Z_{dr}^{-2.08} & Z_{dr} > 1\text{dB, } Z_{hd} > 35 \text{ dBZ and } A_h > 0 \text{ dBZkm}^{-1} \\ 243.2A_h^{0.79} & Z_{dr} \leq 1\text{dB, } Z_{hd} > 35 \text{ dBZ and } A_h > 0 \text{ dBZkm}^{-1} \\ 0.015Z_{hd}^{0.734} & \text{otherwise} \end{cases}$
$R(K_{dp})$	$R = \begin{cases} 32.4K_{dp}^{0.83} & Z_{hd} > 35 \text{ dBZ and } K_{dp} > 0.5 \text{ }^\circ\text{km}^{-1} \\ 0.015Z_{hd}^{0.734} & \text{otherwise} \end{cases}$
$R(K_{dp}, Z_{dr})$	$R = \begin{cases} 46.8K_{dp}^{0.88}Z_{dr}^{-1.31} & Z_{dr} > 1\text{dB, } Z_{hd} > 35 \text{ dBZ and } K_{dp} > 0.5 \text{ }^\circ\text{km}^{-1} \\ 32.4K_{dp}^{0.83} & Z_{dr} \leq 1\text{dB, } Z_{hd} > 35 \text{ dBZ and } K_{dp} > 0.5 \text{ }^\circ\text{km}^{-1} \\ 0.015Z_{hd}^{0.734} & \text{otherwise} \end{cases}$

phased-based algorithms, which are appropriate for estimation of rainfall intensity at the C-Band, were the same as those given in Keenan *et al.* (2001). The third and fourth algorithms, $R(A_h)$ and $R(A_h, Z_{dr})$, used the estimates of attenuation of horizontal reflectivity, A_h , produced by the self-consistent rain profiling method. The fifth and sixth algorithms, $R(K_{dp})$ and $R(K_{dp}, Z_{dr})$, used the specific differential phase, K_{dp} , which is the first derivative of the differential phase shift field with respect to range.

Accuracy of the radar estimated accumulation fields might be improved by calibrating the fields using a raingauge network. Real-time calibration of the rainfall


Fig. 2 Recorded and modelled streamflow hydrographs obtained using $R(Z_{hs})$ radar rainfall algorithm.

fields was simulated by calculating a calibration factor as the average ratio of the raingauge to radar estimated rainfall accumulations for the hour. Only locations where the radar and raingauge accumulations exceeded the greater of 1 mm or two bucket tips were included in the calculation of the calibration factor. The hourly radar accumulation field was then multiplied by calibration factor. Raingauge calibrated rainfall fields were produced for the $R(Z_{hs})$ algorithm rainfall fields using network densities of 150, 300, 600, 1200 and 2400 km² per gauge.

Rainfall estimated using each of the six radar algorithms was used as input to the URBS model for the Georges basin. The URBS model was also run with the single polarization rainfall input, calibrated with each of the five different gauge network densities. The quality of each modelled hydrograph was determined by computing the sum of square errors and coefficient of efficiency (CoE) (Nash & Sutcliffe, 1970) with the recorded hydrograph. URBS model parameter values were set to those determined from the calibration events, except for initial loss from pervious areas, which was calibrated individually for each of the rainfall input fields. However, results were not sensitive to the initial loss parameter, as more than 90% of the runoff in this small flood event was generated from the impervious areas.

RESULTS AND DISCUSSION

Figure 2 shows a typical modelled flood hydrograph produced by the URBS model, in this case with rainfall input from the $R(Z_{hs})$ algorithm. The fit to the observed hydrograph is good, with the total runoff, peak flow and hydrograph shape being well matched. The modelled flood hydrographs produced from all six radar measurement algorithms produce good predictions of the recorded hydrograph, as evidenced by the CoE values given in Table 3. Two of the dual polarization algorithms, $R(A_h)$ and $R(A_h, Z_{dr})$, produce better predictions of the recorded hydrograph than the prediction based upon the single polarization algorithm, $R(Z_{hs})$. This confirms that the rainfall measurement algorithms based upon attenuation fields, as estimated from differential phase shift data, produce more accurate flood hydrographs than those based on conventional reflectivity measurements.

Table 4 shows that calibration with the raingauge network improves the accuracy of the flood hydrographs predicted using single polarization radar data. The CoE generally improves as the network density increases, peaking for a raingauge density

Table 3 Summary statistics for the comparison between the recorded and modelled hydrographs for the different radar rainfall estimation algorithms.

Rainfall algorithm	Basin average rainfall (mm)	Modelled runoff (mm)	Sum of square streamflow errors (m ⁶ s ⁻²)	Coefficient of efficiency
$R(Z_{hs})$	56.12	5.39	1057.4	0.7380
$R(Z_{hd})$	57.05	5.49	1267.5	0.6859
$R(A_h)$	68.11	5.38	936.0	0.7681
$R(A_h, Z_{dr})$	61.16	5.28	993.9	0.7537
$R(K_{sp})$	67.60	5.23	1045.9	0.7409
$R(K_{sp}, Z_{dr})$	65.37	5.20	1090.2	0.7299

Table 4 Summary statistics for the comparison between the recorded and modelled hydrographs using the $R(Z_{hs})$ algorithm with different densities of raingauge calibration networks.

Average raingauge density (km ² per gauge)	Number of calibration raingauges	Basin average rainfall (mm)	Modelled runoff (mm)	Sum of square streamflow errors (m ⁶ s ⁻²)	Coefficient of efficiency
<i>Uncalibrated</i>	0	56.12	5.39	1057.44	0.7380
2400	8	59.94	5.49	887.84	0.7800
1200	16	62.31	5.44	865.02	0.7857
600	32	61.85	5.52	774.93	0.8080
300	64	60.17	5.44	749.18	0.8144
150	128	61.44	5.60	848.12	0.7899

of 1 per 300 km². In this case study, even sparse calibration raingauge networks (2400 km² per gauge) were able to improve the predictions from the $R(Z_{hs})$ fields by more than any of the dual polarization algorithms on their own. Calibration was so effective in this case study because the rainfall was widespread enough to obtain an accurate estimate of the radar rainfall bias from the raingauge networks. Calibration of the best performing dual polarization algorithm field, $R(A_h, Z_{dr})$, with the 300 km² per gauge network produced a less accurate modelled flood hydrograph (CoE = 0.7585) than the single polarization radar data calibrated with the same network.

The results of this case study are conditioned upon the use of raingauge rainfall in calibration of the parameters of the rainfall–runoff model (Troutman, 1983). It is possible that, if radar rainfall were used to calibrate the URBS model, parameter values would adjust themselves so that predictions from the model using radar data would be further improved (Borga, 2002).

Dual polarization rainfall estimation algorithms have their greatest advantage over single polarization algorithms at higher rainfall intensities, typically greater than 10 mm h⁻¹.

It should also be noted that rainfall intensities in this widespread rainfall event were relatively low and that, under these conditions, improvements from dual polarization are likely to be relatively modest. Likewise, raingauge calibration is likely to be most effective in a widespread case, such as this, with a large number of radar and raingauge comparisons. It is likely that convective events, with higher rainfall intensities, will demonstrate the advantages of dual polarization more clearly. Future analysis of other flood events, both convective and widespread, should clarify these issues.

CONCLUSIONS

A case study was analysed of a widespread rainfall event of approximately 2 days duration, producing a small flood in a partially urbanized basin of 354 km² area. A semi-distributed rainfall–runoff routing model was used to predict flood flows from six different radar rainfall measurement algorithms and these were compared to the observed flood hydrograph.

Dual polarization radar rainfall measurement algorithms based upon attenuation fields, as estimated from differential phase shift data, produce more accurate flood

hydrographs than those based on conventional reflectivity based algorithms. However, for this widespread rainfall event, calibration of the reflectivity based rainfall accumulation fields with an hourly reporting raingauge network at a density of 1 per 2400 km² produced a more accurate flood hydrograph than the best of the dual polarization algorithms. Accuracy of the modelled hydrograph improved with calibration network density, peaking at 1 raingauge per 300 km².

It is very likely that dual polarization algorithms will demonstrate clearer advantages in convective rainfall events, where rainfall intensities are greater and raingauge calibration is less effective at removing bias from the reflectivity based rainfall estimates.

Acknowledgements The authors thank Mr Ken Glasson of BMRC for operating and maintaining the C-POL radar during its operation at Badgery's Creek. We also acknowledge Mr Michael Whimpey of BMRC for his assistance in preparation of the C-POL radar data. The authors thank Sydney Water for providing most of the raingauge data used in the research.

REFERENCES

- Austin, P. M. (1987) Relation between measured radar reflectivity and surface rainfall. *Mon. Weath. Rev.* **115**, 1053–1070.
- Borga, M. (2002) Accuracy of radar rainfall estimates for streamflow simulation. *J. Hydrol.* **267**, 26–39.
- Brandes, E. A. (1975) Optimising rainfall estimates with the aid of radar. *J. Appl. Met.* **14**, 1339–1345.
- Bringi, V. N., Keenan, T. D. & Chandrasekar, V. (2001) Correcting C-Band radar reflectivity and differential reflectivity data for rain attenuation: a self-consistent method with constraints. *IEEE Trans. Geosci. Remote Sens.* **39**(9), 1906–1915.
- Carpenter, T. M., Georgakakos, K. P. & Spertslage, J. A. (2001) On the parametric and NEXRAD-radar sensitivities of a distributed hydrologic model suitable for operational use. *J. Hydrol.* **253**, 169–193.
- Carroll, D. G. (1996) *URBS-CM, A Catchment Management and Flood Forecasting Rainfall Runoff Routing Model*. Gutteridge Haskin and Davey, Brisbane, Australia.
- Duan, Q., Sorooshian, S. & Gupta, V. (1992) Effective and efficient global optimisation for conceptual rainfall runoff models. *Water Resour. Res.* **28**(4), 1015–1031.
- Harrold, T. W., English, E. J. & Nicholass, C. A. (1974) The accuracy of radar-derived rainfall measurements in hill terrain. *Quart. J. Roy. Met. Soc.* **100**, 331–350.
- Hitchfeld, W. & Bordan, J. (1954) Errors inherent in the radar measurement of rainfall at attenuating wavelengths. *J. Appl. Met.* **11**, 58–67.
- Keenan, T., Nan, Z., Lei, F., Bringi, V., Nystuen, J. & Whimpey, M. (2001) A comparison of radar rainfall estimators during the South China Sea Monsoon Experiment (SCSMEX) (30th Int. Conf. Radar Meteorology, Munich, Germany), 603–605. Am. Met. Soc.
- Jordan, P. W., Seed, A. W. & Austin, G. L. (2000) Sampling errors in radar estimates of rainfall. *J. Geophys. Res.* **105**(D2), 2247–2257.
- Nash, J. E. & Sutcliffe, J. V. (1970) River flow forecasting through conceptual models 1. A discussion of principles. *J. Hydrol.* **10**, 282–290.
- Ogden, F. L., Sharif, H. O., Senarath, S. U. S., Smith, J. A., Baack, M. L. & Richardson, J. R. (2000) Hydrologic analysis of the Fort Collins, Colorado, flash flood of 1997. *J. Hydrol.* **228**, 82–100.
- Troutman, B. M. (1983) Runoff prediction errors and bias in parameter estimation induced by spatial variability of precipitation. *Water Resour. Res.* **19**, 791–810.
- Yates, D. N., Warner, T. T. & Leavesley, G. H. (2000) Prediction of a flash flood in complex terrain. Part II: A comparison of flood discharge simulations using rainfall input from radar, a dynamic model and an automated algorithmic system. *J. Appl. Met.* **39**, 815–825.
- Zrníć, D. S. & Ryzhkov, A. (1996) Advantages of rain measurements using specific differential phase. *J. Atmos. Oceanic Tech.* **13**, 454–464.